

PAPER

Low-voltage high-reliability MEMS switch for millimeter wave 5G applications

To cite this article: Sudhanshu Shekhar *et al* 2018 *J. Micromech. Microeng.* **28** 075012

View the [article online](#) for updates and enhancements.

Low-voltage high-reliability MEMS switch for millimeter wave 5G applications

Sudhanshu Shekhar^{1,2} , K J Vinoy¹ and G K Ananthasuresh²

¹ Electrical Communication Engineering, Indian Institute of Science, Bengaluru, 560012, India

² Department of Mechanical Engineering, Indian Institute of Science, Bengaluru, 560012, India

E-mail: sudhanshu@iisc.ac.in and shekhar.iisc@gmail.com

Received 19 December 2017, revised 23 February 2018

Accepted for publication 28 March 2018

Published 25 April 2018



Abstract

Lack of reliability of radio-frequency microelectromechanical systems (RF MEMS) switches has inhibited their commercial success. Dielectric stiction/breakdown and mechanical shock due to high actuation voltage are common impediments in capacitive MEMS switches. In this work, we report low-actuation voltage RF MEMS switch and its reliability test. Experimental characterization of fabricated devices demonstrate that proposed MEMS switch topology needs very low voltage (4.8 V) for actuation. The mechanical resonant frequency, f_0 , quality factor, Q , and switching time are measured to be 8.35 kHz, 1.2, and 33 microsecond, respectively. These MEMS switches have high reliability in terms of switching cycles. Measurements are performed using pulse waveform of magnitude of 6 V under hot-switching condition. Temperature measurement results confirm that the reported switch topology has good thermal stability. The robustness in terms of the measured pull-in voltage shows a variation of $0.08 \text{ V } ^\circ\text{C}^{-1}$. Lifetime measurement results after 10 million switching cycles demonstrate insignificant change in the RF performance without any failure. Experimental results show that low voltage improves the lifetime. Low insertion loss (less than 0.6 dB) and improved isolation (above 40 dB) in the frequency range up to 60 GHz have been reported. Measured RF characteristics in the frequency range from 10 MHz to 60 GHz support that these MEMS switches are favorable choice for mm-wave 5G applications.

Keywords: pull-in voltage, low loss, MEMS switch, capacitive switch, RF MEMS, S-parameters

(Some figures may appear in colour only in the online journal)

1. Introduction

Recent developments in mobile and telecommunication systems have shown that MEMS-based devices are promising alternatives to become a part of present as well as upcoming fifth generation (5G) communication systems. It is predicted that MEMS-based RF switches could play an important role in 5G mobile communications [1–3]. However, poor reliability has hindered MEMS switches to meet the commercial standard [4–8]. Among several failure mechanisms in MEMS switches, electrical (ESD, dielectric breakdown, etc) and mechanical (impact force, fatigue, creep, etc) failures are dominant [9–12]. Operational environmental conditions such as temperature, humidity also affect reliability [9, 13, 14]. However, the effect of humidity can be mitigated using hermetic sealing.

RF MEMS switches have been explored extensively over the past two decades due to their exceptional RF characteristics such as low insertion loss, high isolation and almost zero-power consumption [15, 16]. Despite promising features, any switch topology might not be able to overcome the aforementioned failure mechanisms. Therefore, we see that there is a strong need for developing a switch geometry for MEMS switches that results in high reliability, without compromising on their electromechanical and RF performance, to ensure their use in future and present wireless communication systems as well as successfully meeting the commercial standard.

MEMS switches are realized in two different configurations: metal-contact and capacitive-shunt type. A capacitive MEMS switch uses a thin-layer (of almost 100 nm) of dielectric. The dielectric layer avoids the direct contact between the top and

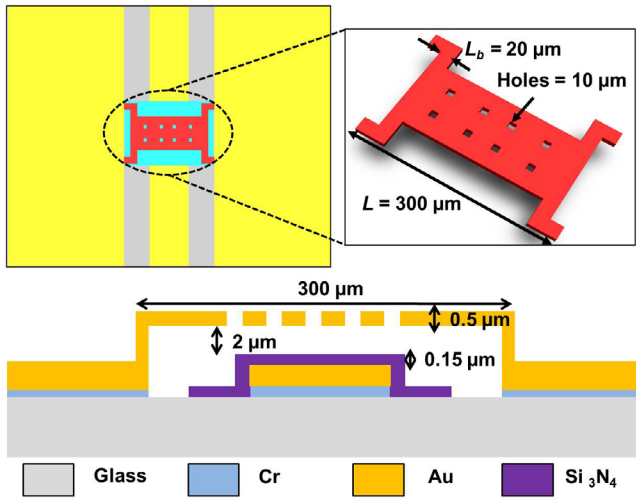


Figure 1. Schematics of L-support beams capacitive RF MEMS switch.

the bottom electrodes of the switch. In addition, the presence of dielectric layer increases the capacitance ratio and hence the figure-of-merit (FoM) of MEMS switches. The dielectric strongly depends on the actuation voltage used to achieve *ON* and *OFF* of the RF signal passing through the transmission line. The reliability of capacitive MEMS switches is largely affected by dielectric charging and dielectric breakdown at high actuation voltage. However, the charge-trapping mechanism during charging/discharging process is not yet fully understood [17]. The erratic behavior of dielectric due to high actuation voltage is considered to be one of the reasons behind the failure of capacitive MEMS switches. To avoid the failure due high actuation voltage and mechanical shock, various strategies have been reported [18–21]. By reducing actuation voltage, the lifetime expectancy of these switches can be extended.

This paper is an extension of our previous work [22, 23]. In this work, we investigate the reliability and report the DC, RF, lifetime and thermal measurement of capacitive RF MEMS switches. These MEMS switches are successfully tested in the frequency range up to 60 GHz with excellent RF features at low-power (i.e. below 1 mW) under hot switching conditions. Thermal measurements are performed up to 100 °C.

2. Switch design and fabrication

Figure 1 presents the top and the cross-section view along with the dimensions of the MEMS switch. The topology of switch-beam is crucial to enhance the overall performance in terms electromechanical and RF performance. We considered the switch topology, as shown in the figure 1, due its salient features in terms of low-stiffness which results in low pull-in voltage; low- Q factor which results in reduced settling time after the release; and reasonable switching time at low-voltage. The switch topology uses four L-shaped beams attached to the central part to achieve low pull-in voltage. This topology results in low-stiffness, k , of 1.34 N m^{-1} . Finite element (FE) simulation results indicate that the proposed topology needs

less than 5V for actuation. In addition, our design with fewer holes of adequate dimension helps achieve low quality factor, Q , and improved switching dynamics during pull-in and release (when the actuation voltage, V_S , is removed and the switch membrane returns to its un-deformed state) [23].

The switch is implemented in shunt-configuration suspended at a height of $2 \mu\text{m}$ above a 50Ω CPW transmission line. CPW transmission lines are fabricated using $0.5 \mu\text{m}$ sputtered gold (Au). A thin layer (150 nm) of Si_3N_4 is used as dielectric layer underneath the central part of the switch-beam to avoid the direct contact. The fabricated MEMS switches are released using CO_2 critical-point-dryer to avoid stiction due to surface tension. Pyrex glass is used as a substrate and four-mask surface-micromachining process is used for fabrication. The fabrication process was developed at the Centre for Nano Science and Engineering (CeNSE) at Indian Institute of Science (IISc). Figures 2 and 3 show the process flow and SEM image of the fabricated MEMS switch. More details on the design, modeling, and fabrication are discussed in our earlier work [22, 23].

3. Experiments

The fabricated MEMS switches were diced and released using wet-release process for further characterization. Preliminary mechanical and electrical measurement reported in this section were conducted to investigate electrical and RF performance of the fabricated devices. All the measurements were conducted under standard temperature (25 °C) and normal pressure (101 kPa) conditions. Experimental results and details of measurements are presented next.

3.1. DC and mechanical characterization

Figure 4 presents the capacitance versus voltage (C-V) measurement result. DC-sweep method was used to measure pull-in and pull-up voltages. A Semiconductor Parametric Analyzer (Agilent 4248) was used. The actuation voltage is swept from 0 V-to-10 V-to-0V in steps of 100 mV. Measured pull-in and pull-up voltage voltages were found to be 4.8V and 2.8V, respectively. The capacitance values in up and down-states were measured to be 0.08 pF and 0.7 pF.

PolyTech MSA-500 (Micro System Analyzer), Laser Doppler Vibrometer (LDV) was used for the experimental evaluation of mechanical properties such as resonant frequency, f_0 , Q -factor, and switching dynamics. An LDV uses Doppler shift to measure the displacement as well as velocity. He-Ne laser having wavelength of 633 nm and a laser-beam of spot size of $1 \mu\text{m}$ was used to scan the region of interest of the device under test (DUT). Figure 5 presents the frequency response of the MEMS switches measured using a 0.6V AC superposed with 2V DC signal. The insets in the figures show the optical micrographs and the LDV-constructed motion images of the switch.

We used LDV for the estimation of switching and release times. The dynamic behavior of the switches were monitored by providing a train of square-pulse voltage along with offset

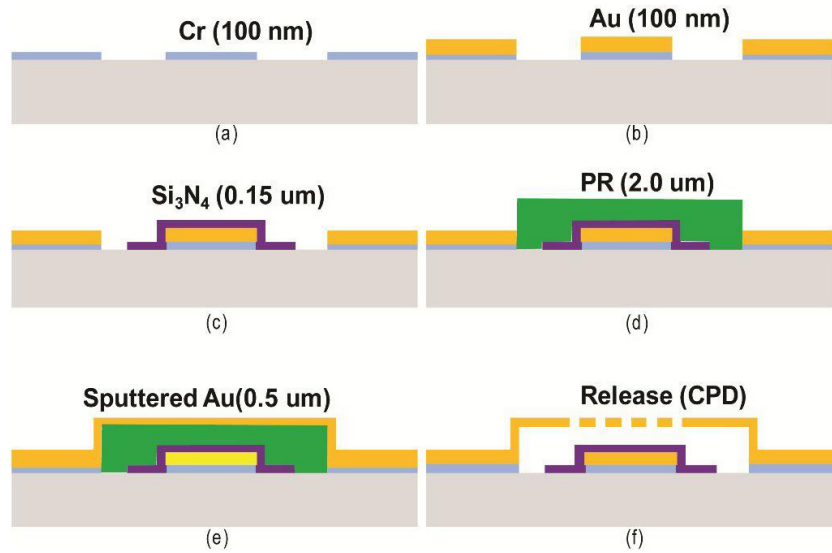


Figure 2. Fabrication process flow.

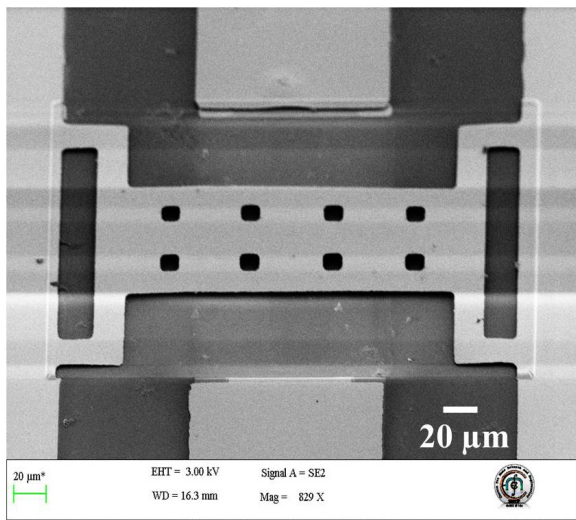


Figure 3. Scanning electron microscope image of a fabricated MEMS switch.

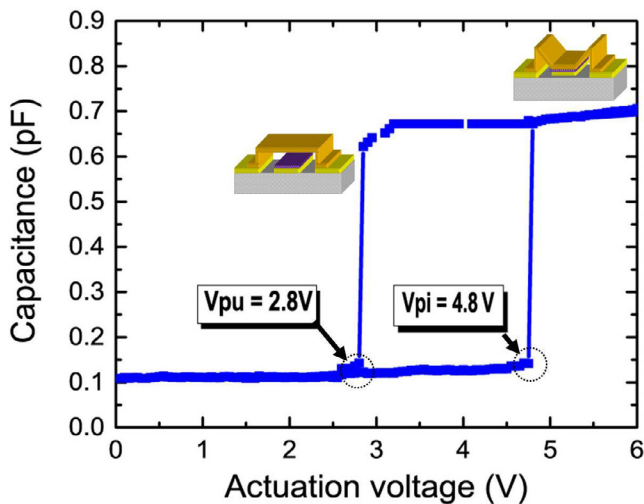


Figure 4. The capacitance versus voltage plot showing the pull-in characteristic of the switch.

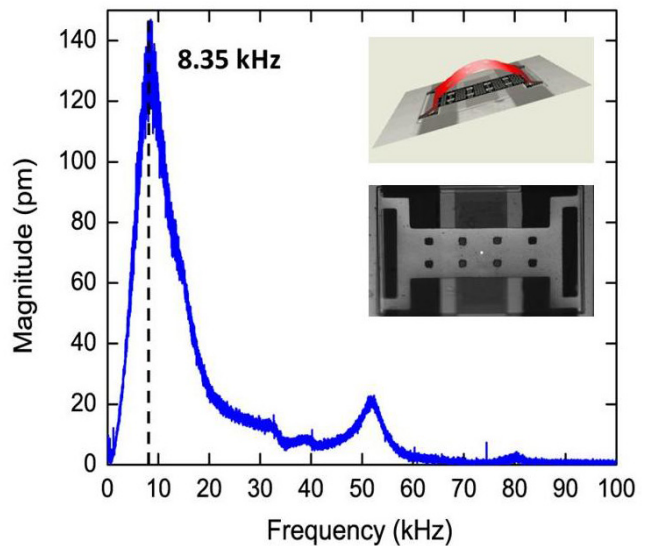


Figure 5. Mechanical resonant frequency response captured using LDV.

voltage level. Measurements were performed under normal atmospheric conditions. A square wave signal of cyclic frequency 1 kHz with 50% duty cycle was used for the actuation. Since, these switches need low-actuation voltage (less than 5V). The amplitude of the square wave was varied from 4.0V to 5.0V in steps of 200 mV to observe the switching and release characteristics. The switching dynamics of switches were studied for three different conditions of the actuation voltage i.e. (i) $V_S < V_{PI}$, (ii) $V_S = V_{PI}$, and (iii) $V_S > V_{PI}$. Figure 6 presents the measured switching dynamics for different actuation voltages. We observed that switches show low-settling (less than 1% of the initial gap, g_0) after the release (i.e. when $V_S = 0$ V) and reduced bouncing of the switch membrane during the contact (see figure 6). These features can be attributed to the low Q -factor which is 1.24. Release times were also measured and found to be less than 20 μ s. Tables 1 and 2 summarizes the FE simulation and measured

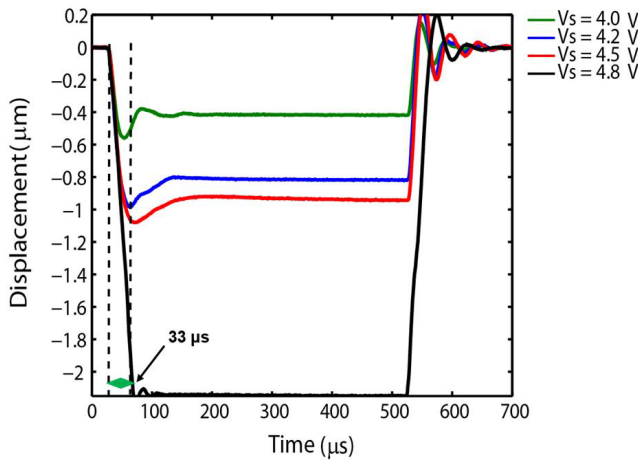


Figure 6. Switching and release time response under LDV.

Table 1. Comparison between FEM-simulated and measured results.

Parameters	FEM	Measured
V_{PI} (V)	4.5	4.8
V_{PU} (V)	1.5	2.8
C_{up} (pF)	0.01	0.08
C_{dn} (pF)	1.1	0.69
f_0 (kHz)	8.29	8.35
Q	—	1.24

Table 2. Switching and release times at different actuation voltage.

Actuation vol. (V)	Pull-in time (μ s)	Pull-up time (μ s)
$V_s = V_{PI}$	33	<20
$V_s = 1.2 V_{PI}$	31	<20
$V_s = 1.4 V_{PI}$	18	<20

results. In table 2, switching and release times are represented as pull-in and pull-up times, respectively. Since, pull-up or release, which is completely a mechanical phenomenon i.e. the switch regains its original/un-deflected shape due to the stored mechanical energy, the release time measured same for all the three cases.

3.2. RF characterization

Agilent E8361A Vector Network Analyzer (VNA) and cascade probe station with 200 μ m pitch coplanar (GSG) probes were used to measure S-parameters of the fabricated MEMS switches. On-wafer measurements were performed using Short-Open-Load-Thru (SOLT) calibration technique under normal atmospheric conditions.

Figures 7 and 8 present the measured and simulated S-parameter results in up- and down-states. Measured insertion loss (in up-state i.e. un-actuated position) is found to be less than 0.15 dB, 0.4 dB and 0.6 dB at 20 GHz, 40 GHz and 60 GHz, respectively. The measured return loss (up-state) is better than 12 dB across the frequency range up to 60 GHz. In the down-state i.e. actuated position, the isolation is measured

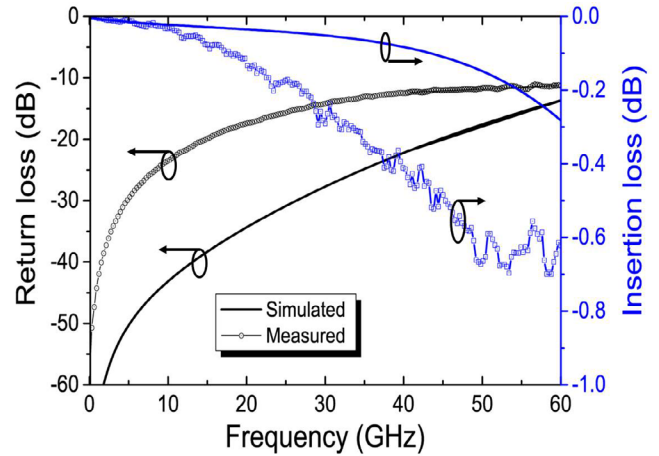


Figure 7. Simulated and measured S-parameters in up-state position.

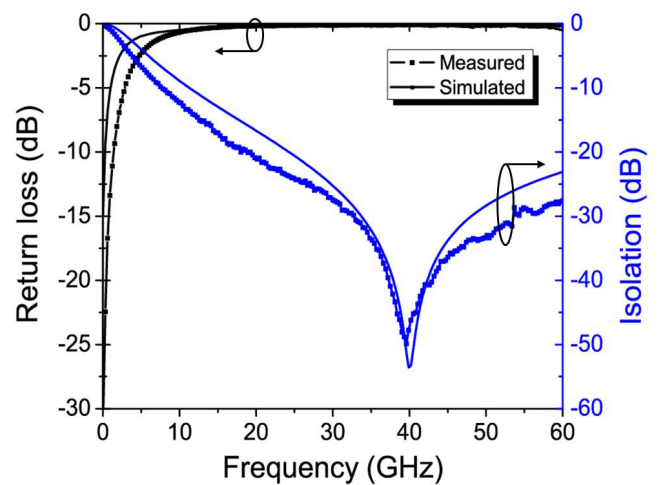


Figure 8. Simulated and measured S-parameters in down-state position.

better than at 40 dB at 40 GHz as shown in figure 8. Measured RF characteristics of these MEMS switches, in the frequency range of above 20 GHz, suggests that these switches can readily be used in mm-wave 5G applications.

3.3. Thermal measurement

Thermal stability is another criterion which defines the reliability of MEMS switches. The purpose of this experiment was to evaluate the thermal stability of the fabricated MEMS switches. The robustness of fabricated MEMS switches was tested at elevated temperature in the range of 25 °C to 100 °C. We conducted thermal analysis using DC-sweep method using Parametric Analyzer to study the effect of temperature on the pull-in voltage. A temperature controller is attached to the chuck of the probe station and varied the temperature from 25 °C to 100 °C and corresponding capacitance-voltage (C-V) characteristics were measured.

Figure 9 presents the measured capacitance versus voltage (C-V) plot showing the shift in pull-in voltage with temperature. Measured pull-in voltages at 25 °C and 100 °C show

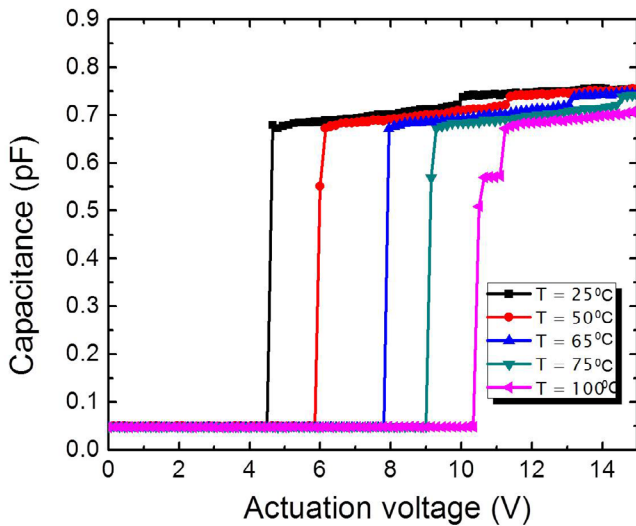


Figure 9. Measured C-V plot showing shift in pull-in voltage over temperature.

a shift of almost 6V with a nominal variation of $0.08\text{V } ^\circ\text{C}^{-1}$ over the temperature up to 100°C . The change in up-state capacitance, C_{up} , was found to be insignificant (less than 1%). However, a slight variation in the down-state capacitance, C_{dn} , was apparent. The measurement results show a positive shift in the pull-in voltage with rise in the operational temperature. Such effect, in case of fixed-fixed geometry based RF MEMS switches, is previously reported [24, 25]. The biaxial stress is induced post fabrication in the switch beam depends on the operational temperature. Therefore, the observed shift in the pull-in voltage can be attributed to the thermally tensile-stress induced in the thin-film at high temperature as shown in figure 9.

Furthermore, we performed similar measurement on various devices to see the study the effect of temperature. Measured results of a set of five devices on the same wafer are shown in figure 10. Between two consecutive measurements (at different temperatures) overnight recovery time was given. Tests were performed on multiple devices at various locations on a 4 inch wafer. Measured results showed a similar trend. We did not perform negative thermal measurement as these were un-packaged devices.

4. Reliability measurements

The reliability of a MEMS switch is defined in terms of the number of switching cycles it performs without failure under various testing conditions. For a capacitive RF MEMS switch, it should be close to or above 1 billion cycles. Though, reliability of MEMS switches is still an open issue, one of the potential failure mechanisms is the dielectric charging due to high actuation voltage. Therefore, reduce the actuation voltage and hence increase the longevity of capacitive MEMS switches, we design the switch that needs very low voltage for actuation.

The lifetime measurements on fabricated MEMS switches were performed using in-house developed measurement setup

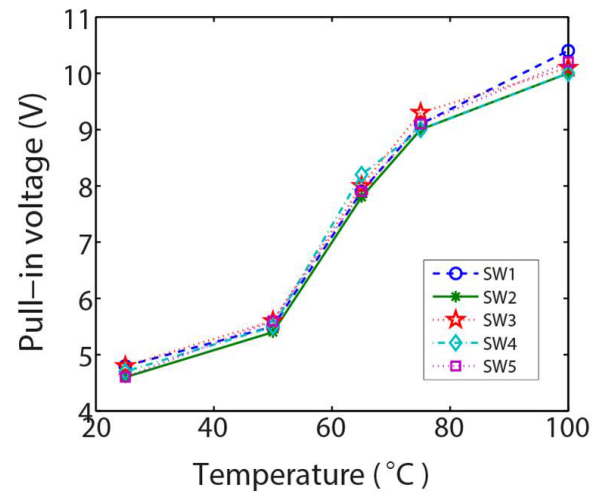


Figure 10. Measured pull-in voltage as a function of temperature for five switches.

based on LabView for efficient automated measurement. The complete measurement setup is shown in figure 11. The devices were tested under ‘hot switching’ condition. In hot-switching test, the input RF signal is continuously ‘ON’ along with the actuation voltage. Because of the instrument’s limitation, these devices were tested below 1 mW in the frequency range up to 60 GHz.

Agilent E8361A Vector Network Analyzer (VNA) used to provide RF signal up to 60 GHz and to measure the S-parameters in the actuated and un-actuated states. Agilent 811501A Pulse Function Arbitrary Signal Generator was used to provide unipolar square pulse to actuate the devices under test. The output of the function generator is a train of square pulse voltages which is fed to the DC-port of the VNA. These trains of pulse voltages provide adequate actuation voltage that actuates the switch (DUT) in order to measure the RF response in actuated and un-actuated states. The magnitude of the actuation pulse was kept at $1.1\text{--}1.2 V_{PI}$ to ensure pull-in happens within finite time.

Figures 12 and 13 present measured S-parameters in up- and down-state conditions after 10 million switching cycles performed on the fabricated devices. The S-parameters were measured after 10^1 , 10^2 , 10^3 , 10^4 , 10^5 , 10^6 , and 10^7 cycles. Since, the VNA response time is slower (of the order of few milliseconds) than the switching response time of MEMS devices. Therefore, the actuation pulse was kept high for about 1 min in the hold-down position after every specified switching cycle to extract the measured S-parameters. Measured RF performance even after 10 million cycles were stable without much variation. All these instruments were connected through GP-IB cables and controlled using LabView-based program to measure the S-parameters after a specific number of switching cycles.

We also performed measurement to observe any significant change or shift in the pull-in voltage after number of switching cycles. Figure 14 presents the comparison of measured C-V response before and after 10 million cycles. Insignificant shift in the pull-in and pull-out voltage confirms that low actuation voltage does add much to the dielectric charging as well as

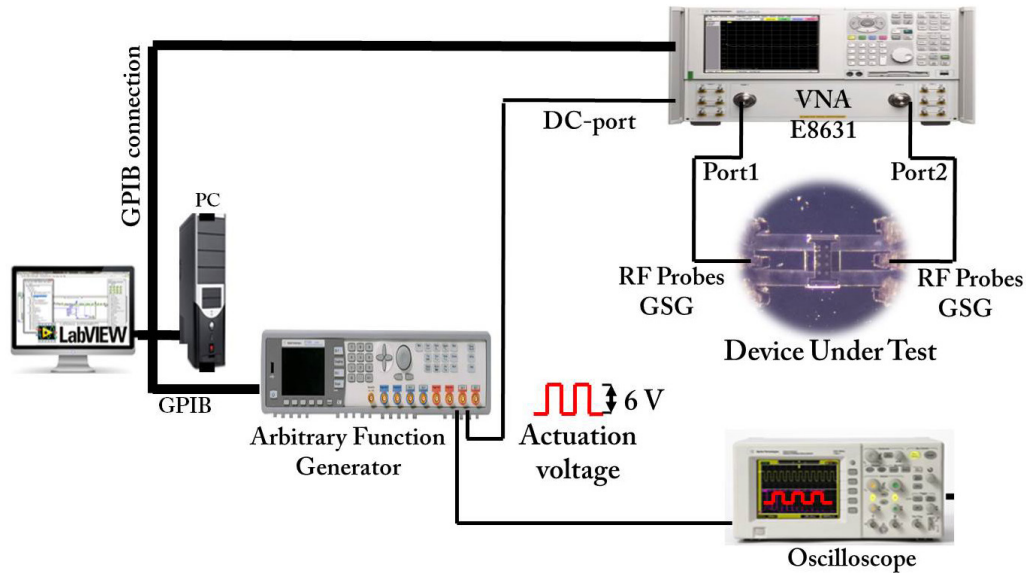


Figure 11. Measurement setup for lifetime measurement.

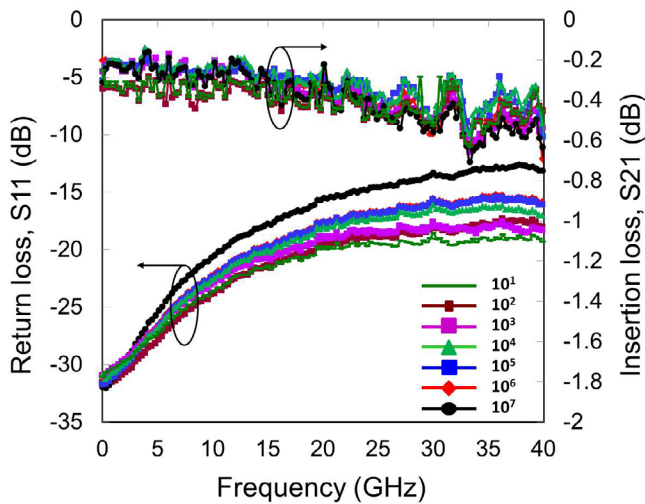


Figure 12. Measured S -parameters in up-state after number of cyclic operations.

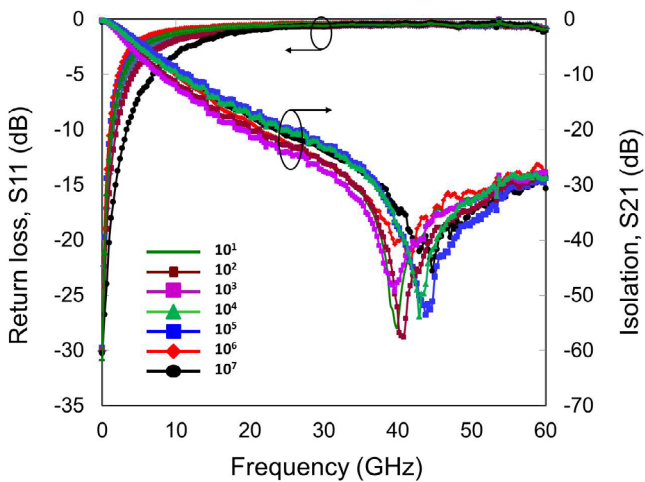


Figure 13. Measured S -parameters in down-state after number of cyclic operations.

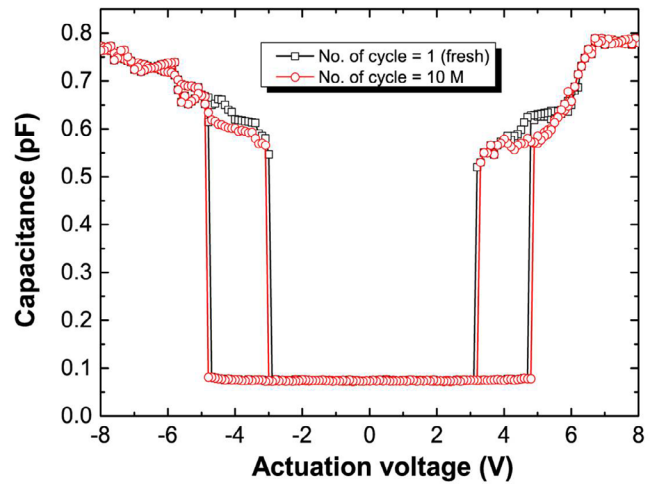


Figure 14. Measured C-V response after and before 10M switching cycles.

charge trapping. This results suggest that how the lifetime of a capacitive MEMS switch can be improved significantly.

5. Results and discussion

DC, RF, thermal, and lifetime characterization are conducted to evaluate the reliability of the fabricated capacitive RF MEMS switches. We noted that the dielectric charging effect can be minimized and hence the longevity of capacitive MEMS switches can be enhanced by ensuring low-actuation voltage. To perform a large number of switching cycles (>millions), for reliability analysis, the experimentation takes days to complete. Therefore, to avoid time consuming measurement, automated measurement setup is required. We performed the measurement using LabView-based automated measurement setup shown in figure 11. The frequency sweep during S -parameters measurement using vector network analyzer (VNA), it takes 6.4ms to perform one measurement.

To perform a set of measurements with the cyclic frequency of 1 kHz and 50% duty cycle, it takes about 28 h to complete 10 million switching cycles. The appropriate pulse duration not only helps in preventing the charge trapping but also provides adequate time for the oscillation, which occurs after the release, to damp out before the each transition. Trapped charges in the dielectric layer can influence the measurement results by shifting switching and release times between two consecutive actuation pulses. Furthermore, increase in duty cycle increases the actuation time which further increases the charge-accumulation. However, the charge trapping phenomenon can be avoided by introducing sufficient delay between successive measurements. Therefore, during the measurement, we kept the actuation voltage at high and low-level for equal period of time i.e. for 1 ms. Time-averaging was also performed to improve the signal-to-noise ratio for the accuracy of the measurement. Measurement results ensure a delay of 1 ms between the high and the low pulses is sufficient to avoid charge-trapping.

As per author's knowledge, the highest switching time reported so far is 914 billion switch cycles [26]. It took approximately 18 months to complete the measurement of aforementioned number of switching cycles. Since, no major shift and degradation was observed, in the present work, measurement was discontinued after 3 d due to time constraint. Repeated measurements up to 10 million cycles did not lead to any degradation in the RF performance. This establishes low actuation voltage helps in enhancing the longevity of capacitive RF MEMS switches. The measurement results of the reliability test conducted in this work confirm that with a thin-metal membrane ($0.5 \mu\text{m}$) and low-voltage high-reliability can be realized for MEMS switches. Future deployments of 5G in 2018 in USA is aiming the frequency band of 27.5–28.35 GHz and 37–40 GHz; European Union for 24.25–27.5 GHz, and for commercial deployments from 2020; while China is targeting 24.25–27.5 GHz and 37–43.5 GHz [27]. Measured RF performance, i.e. return loss less than 12 dB; low-insertion of -0.6 dB; and isolation better than 40 dB, in the frequency range from 20–40 GHz, supports that our MEMS switches are good candidates and can be implemented in 5G (higher band) applications.

As noted, operational temperature, is another important factor that decides the reliability of MEMS devices. We investigated the effect of temperature on fabricated MEMS switches. The purpose behind conducting variable temperature measurements was to investigate the thermal sensitivity of fabricated devices. Measurement results show that our MEMS switches are not very sensitive to temperature variations. The variation of $0.08 \text{ V } ^\circ\text{C}^{-1}$ over the temperature range of $75 \text{ }^\circ\text{C}$ was reported. Slight variation in the pull-in voltage was noted. The noted variation in the pull-in voltage, as shown in Fig 12, can be attributed to the tensile-stress induced in thin-film at elevated temperatures. Furthermore, the repeated measurements confirm that with $0.5 \mu\text{m}$ thick-film of gold with fewer number of etch holes in the switch membrane helps achieve thermally stable MEMS switches over a wide range.

6. Conclusions

We presented DC, RF and thermal measurements of capacitive RF MEMS switches along with reliability tests. These switches require low voltage (less than 5 V) for actuation. Up to 10 million switching cycles do not show any degradation in the RF performance under hot switching condition. Furthermore, variation in the pull-in voltage over the range of up to $100 \text{ }^\circ\text{C}$ was found to be less than $0.08 \text{ V } ^\circ\text{C}^{-1}$. The experimental results presented in this work justify that the approach to achieve low-actuation voltage considering proposed switch topology helps in enhancing the longevity of capacitive RF MEMS switches. The switching and release times of the switch are $33 \mu\text{s}$ and less than $20 \mu\text{s}$; quality-factor, Q , of 1.24, which is recommended for RF MEMS switches ($Q \sim 1$), and mechanical resonance frequency, f_0 , is 8.35, respectively. Furthermore, RF measurement results explain the suitability of these MEMS switches for mm-wave 5G applications.

Acknowledgment

The authors would like to thank facility technologists Maniknatha, Amit, Varadharaja Perumal at the Centre for Nano Science and Engineering (CeNSE) at Indian Institute of Science (IISc) for their support in fabrication and characterization.

ORCID iDs

Sudhanshu Shekhar  <https://orcid.org/0000-0001-6355-974X>

References

- [1] Iannacci J and Tschoban C 2017 RF-MEMS for future mobile applications: experimental verification of a reconfigurable 8-bit power attenuator up to 110 GHz *J. Micromech. Microeng.* **27** 044003
- [2] Iannacci J, Huhn M, Tschoban C and Pötter H 2016 RF-MEMS technology for 5G: series and shunt attenuator modules demonstrated up to 110 GHz *IEEE Electron Device Lett.* **37** 1336–9
- [3] Iannacci J, Huhn M, Tschoban C and Pötter H 2016 RF-MEMS technology for future mobile and high-frequency applications: reconfigurable 8-bit power attenuator tested up to 110 GHz *IEEE Electron Device Lett.* **37** 1646–9
- [4] Goldsmith C, Maciel J and McKillop J 2007 Demonstrating reliability *IEEE Microw. Mag.* **8** 56–60
- [5] de Wolf I 2006 Reliability of MEMS *7th Conf. on Thermal, Mechanical and Multiphysics Simulation and Experiments in Micro-Electronics and Micro-Systems, EuroSime* pp 1–6
- [6] Rebeiz G M, Patel C D, Han S K, Ko H and Kevin M J 2013 The search for a reliable MEMS switch *IEEE Microw. Mag.* **14** 57–67
- [7] Dhennin J, Djemel L and Pressecq F 2015 How to evaluate the reliability of MEMS devices without standards *DTIP MEMS MOEMS—Symp. on Design, Test, Integration and Packaging of MEMS and MOEMS* pp 1–3

- [8] Lee C 2016 Reliability and failure analysis of MEMS/NEMS switch *IEEE 23rd Int. Symp. on the Physical and Failure Analysis of Integrated Circuits* pp 408–13
- [9] Zhu Y and Espinosa H D 2004 Effect of temperature on capacitive RF MEMS switch performance—a coupled-field analysis *J. Micromech. Microeng.* **14** 1270–9
- [10] Tazzoli A, Peretti V and Meneghesso G 2007 Electrostatic discharge and cycling effects on ohmic and capacitive RF-MEMS switches *IEEE Trans. Device Mater. Rel.* **7** 429–37
- [11] Lamhamdi M, Pons P, Zaghoul U, Boudou L, Coccetti F, Guastavino J, Segui Y, Papaioannou G and Plana R 2008 Voltage and temperature effect on dielectric charging for RF-MEMS capacitive switches reliability investigation *Microelectron. Reliab.* **48** 1248–52
- [12] Huang Y, Vasan A S, Doraiswami R, Osterman M and Pecht M 2016 MEMS reliability review *IEEE Trans. Device Mater. Rel.* **12** 482–93
- [13] Spengen W M 2012 Capacitive RF MEMS switch dielectric charging and reliability: a critical review with recommendations *J. Micromech. Microeng.* **22** 074001
- [14] Wang L, Tang J Y and Huang Q A 2013 Effect of environmental humidity on dielectric charging effect in RF MEMS capacitive switches based on C-V properties *J. Microelectromech. Syst.* **22** 637–45
- [15] Yao J J 2000 RF-MEMS from a device perspective *J. Micromech. Microeng.* **10** R9–38
- [16] Rebeiz G M 2003 *RF-MEMS Theory, Design, and Technology* (Hoboken, NJ: Wiley)
- [17] Zaghoul U, Papaioannou G, Bhushan B, Coccetti F and Plana R 2011 On the reliability of electrostatic NEMS/ MEMS devices: review of present knowledge on the dielectric charging and stiction failure mechanisms and novel characterization methodologies *Microelectron. Reliab.* **51** 1810–8
- [18] Goldsmith C, Forehand D, Yuan X B and Hwang J 2006 Tailoring capacitive switch technology for reliable operation *Proc. Govt Microcircuit Appl. Critical Tech. Conf.* pp 1–4
- [19] Czapslewski D A, Christopher W D, Sumali H, Massad J E, William D C and Christopher P T 2006 A soft-landing waveform for actuation of a single-pole single-throw ohmic RF-MEMS switch *J. Microelectromech. Syst.* **15** 1586–94
- [20] Ou K S, Chen K S, Yang T S and Lee S Y 2011 Fast positioning and impact minimizing of MEMS devices by suppression of motion-induced vibration by command-shaping method *J. Microelectromech. Syst.* **20** 128–39
- [21] Small J, Fruehling A, Garg A, Liu X and Peroulis D 2012 DC-dynamic biasing for >50× switching time improvement in severely underdamped fringing-field electrostatic MEMS actuators *J. Micromech. Microeng.* **22** 125029
- [22] Shekhar S, Vinoy K J and Ananthasuresh G K 2014 Design, fabrication and characterization of capacitive RF-MEMS switches with low pull-in voltage *Proc. IEEE Int. Microw. RF Conf. (IMaRC)* pp 182–5
- [23] Shekhar S, Vinoy K J and Ananthasuresh G K 2017 Surface-micromachined capacitive RF switches with low actuation voltage and steady contact *J. Microelectromech. Syst.* **26** 643–52
- [24] Goldsmith C and Forehand D 2005 Temperature variation of actuation voltage in capacitive MEMS switches *IEEE Microw. Wireless Compon. Lett.* **15** 718–20
- [25] Reines I and Rebeiz G M 2011 Thin-film aluminum RF-MEMS switched capacitors with stress tolerance and temperature stability *J. Microelectromech. Syst.* **20** 193–203
- [26] Newman H S, John L, Judy D and Maciel J 2008 Lifetime measurements on a high-reliability RF-MEMS contact switch *IEEE Microwave Wireless Compon. Lett.* **2** 100–2
- [27] Barrett J 2017 <https://gsacom.com/5g-spectrum-bands>